Proceedings of the Estonian Academy of Sciences,
2017, **66**, 4, 455–461
https://doi.org/10.3176/proc.2017.4.23
Available online at www.eap.ee/proceedings

FUNCTIONAL MATERIALS

Luminescence properties of chlorine molecules in glassy SiO_2 and optical fibre waveguides

Linards Skuja[a*], Koichi Kajihara[b], Krisjanis Smits[a], Kalvis Alps[c], Andrejs Silins[a], and Janis Teteris[a]

[a] Institute of Solid State Physics, University of Latvia, Kengaraga 8, LV-1063 Riga, Latvia
[b] Department of Applied Chemistry, Graduate School of Urban Environmental Sciences, Tokyo Metropolitan University, 1-1 Minami–Osawa, Hachioji, 192–0397 Tokyo, Japan
[c] Light Guide Optics International, Ltd., P.O. Box 1, LV-5316 Livani, Latvia

Received 8 May 2017, revised 15 July 2017, accepted 22 Aug 2017, available online 30 November 2017

Abstract. Glassy SiO_2 is the basic material for optical fibre waveguides and manufacturing-induced Cl impurities reduce their transparency in UV spectral range. This work reports in-depth study/spectroscopic parameters of the near-infrared (1.23 eV) low-temperature photo-luminescence (PL) of interstitial Cl_2 molecules in SiO_2. The zero-phonon line position was estimated at 2.075 eV on the basis of anharmonicity of Cl_2 PL vibronic data. The vibronic sub-bands are broadened by coupling to phonons and by an additional contribution from the glassy disorder. The Huang–Rhys factor is ≈13. The PL decay time is between 1 and 10 ms in the temperature range 100 K–13 K and can be reproduced by 3 exponents. Cl_2 PL retains relatively high quantum yield and its characteristic structured shape, when the temperature is increased from 13 K to the liquid nitrogen temperature. This allows using it conveniently as a high-sensitivity diagnostic tool for detecting Cl_2 impurities in optical fibre waveguides. Time-resolved measurements of optical fibre waveguides indicate that the lower detection limit is below 10^{10} Cl_2/cm^3.

Key words: photonics, amorphous SiO_2, luminescence, Cl_2 impurities, optical fibres.

1. INTRODUCTION

Synthetic glassy SiO_2, also called silica glass, quartz glass, amorphous SiO_2, is the key material for optical fibre waveguides, ultraviolet (UV), high power laser and radiation-resistant optics. For these applications, the purity of the material is of utmost importance and parts-per-billion level has been reached for most impurities. One of the remaining exceptions is chlorine. It is left in glassy SiO_2 due to the synthesis process by oxidizing $SiCl_4$ or by the "drying" step where the silanol (bound hydroxyl ≡Si–O–H) groups are removed in Cl_2 ambient. Typical Cl concentrations are 1–1000 ppm. The "dry" (low silanol content) glasses tend to have larger concentrations of Cl compared to the "wet" SiO_2 glasses. Only few types of synthetic SiO_2 glass, obtained by sol–gel technology [1] or from silicon-organic raw-materials have Cl concentrations below 1 ppm (e.g., commercial types Suprasil UVL or Corning 7979, produced from octamethylcyclotetrasiloxane OMCTS, $[(CH_3)_2SiO]_4$).

The main chemical form of chlorine in glassy SiO_2 is silicon chloride group (≡Si–Cl). It worsens the optical transparency of silica in the deep-UV and vacuum-UV spectral regions [2]. The Cl impurities increase the irradiation-induced attenuation of optical fibres (e.g.,

* Corresponding author, skuja@latnet.lv

ref. [3]). The low-Cl-content (<20 ppm) dry "KS–V4" silica [4] radiation-resistant fibres are considered among the best for visible spectral range optical plasma diagnostics in ITER reactor. In the presence of interstitial O_2 molecules Si–Cl groups can be transformed to interstitial Cl_2 molecules [5], which give rise to 328 nm (3.78 eV) optical absorption band [2]. This absorption band is typically observed in many commercial optical fibre waveguide cables designed for the near-infrared (NIR) applications.

We have recently reported [6] that interstitial Cl_2 molecules in glassy SiO_2 give rise to a NIR-range photoluminescence (PL) band at 1.2 eV, distinguished by a characteristic vibronic structure due to a coupling to the Cl–Cl vibrations. The luminescence is observable at temperatures below 140 K. Since this PL: (1) retains a significant intensity at the liquid nitrogen temperature, 78 K; (2) has characteristic shape, distinguishing it from other broad and non-structured luminescence bands in glassy SiO_2; (3) has long lifetime (≥1 ms) enabling time-resolved separation of the emitted light, it could be possibly used as a high sensitivity tool to detect the presence of Cl_2 and its photochemical reactions in optical fibre waveguides. The purpose of the present work is to obtain further spectroscopic characteristics of interstitial Cl_2 molecules in glassy SiO_2 and to test their detection in optical fibre waveguides.

2. MATERIALS AND METHODS

2.1. Samples

Conventional "bulk" samples of glassy SiO_2 and optical fibres were studied. The bulk samples were of size 5 mm × 10 mm × 12 mm^3 and had all faces optically polished. They contained 7×10^{17} Cl_2/cm^3, as determined by the amplitude of the 328 nm optical absorption (OA) band, using the OA peak cross section for isolated Cl_2 molecules [7]. Two 1 m long samples of multimode optical fibres were studied: UV-optimized fibre for 1200–200 nm region (core diameter 600 μ) and NIR–to–visible range optimized fibre (2200–400 nm, core diameter 400 μ). Both fibres had undoped silica core and fluorine doped cladding, numerical aperture was 0.22. UV fibre contained ≈800 ppm SiOH groups, while the NIR fibre contained less than 5 ppm SiOH.

2.2. Instrumentation

The PL of the bulk sample was measured in He-refrigerator cryostat in the conventional right-angle geometry. Excitation sources were 374.71 nm GaN diode laser (Oxxius OXV 375), 473 nm DPSS laser (Lasever) or 150 W Xe lamp (Oriel) through 200 mm double monochromator (AMKO LTI). A mechanical chopper was placed into the excitation beam for time-resolved measurements. CW-mode and time-resolved emission was measured with 300 mm spectrograph (Andor Shamrock 303i, 150 l/mm grating) and cooled Si CCD (Andor DU971–UVB). In time-resolved mode, the CCD exposure was synchronized with the chopper dark periods. Prior to the exposure, a CCD cleanout cycle had to be performed, introducing ≈4 ms jitter in readout timing relative to the chopper signal. PL decay kinetics was obtained using Hamamatsu R955 photomultiplier and FastComtec 7882 multichannel counter.

The PL of fibre-optic waveguides was measured in the back-scattering configuration (Fig. 1). For low-temperature measurement, ≈80 cm of the 100 cm long fibre was immersed in liquid nitrogen. A careful selection of the filters blocking the excitation laser light was necessary to reduce the admixture of their luminescence to the measured PL spectrum.

PL emission spectra at λ >850 nm were distorted by etaloning (light interference fringes) in the back-thinned CCD and by 2nd overtone absorption of SiO–H vibration at 930 nm in the optical fibre cable used to input light into the spectrograph. In the bulk sample PL measurements, these distortions were corrected by normalizing against the spectrum of a calibrated halogen lamp (Ocean Optics DH2000–CAL). In the case of optical fibre PL, this calibration was inefficient due to different patterns of CCD illumination during measurements and calibration, which yielded different positions of interference fringes on CCD. Therefore, these PL spectra are presented in uncorrected form.

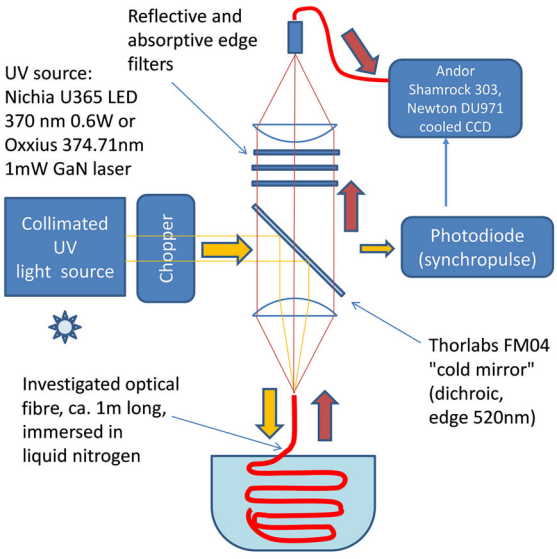

Fig. 1. Setup for investigation of low-temperature near-infrared photoluminescence of optical fibre waveguides.

The attenuation of the optical fibres was measured using a CCD spectrograph (Hamamatsu 10082CAH, spectral resolution 1 nm) and a D_2/halogen light source (Ocean Optics DH2000), both equipped by solarization-resistant 100 μ core fibre cables with SMA–1 connectors. The light was injected into, and extracted from the fibre under investigation, (core diameter 400 or 600 μ) by placing its ends nearly in contact with the centres of the end surfaces of SMA–1 connectors of both cables. After taking the spectrum, the middle fibre was removed, the two fibres were connected by SMA–1 adapter, and the reference spectrum through two fibres was recorded.

3. RESULTS

The optical absorption spectra of the NIR fibre and of the bulk sample show band at 3.78 eV with amplitudes 0.00311 and 0.17 cm^{-1}, (1.35 and 74 db/m), respectively (Fig. 2). This band is absent in the UV fibre. NIR fibre shows as well bands at 5.0 eV and 5.8 eV due to divalent Si atoms ("oxygen deficiency centres") and Si dangling bonds ("E′ centres") [8,9].

The inset of Fig. 3 (top curve) shows the PL spectrum of the bulk sample measured at T = 13 K and 473 nm excitation. The non-structured part of this spectrum can be approximated by a Gaussian (peak 1.215 eV, FWHM 0.39 eV). Subtracting it from the measured spectrum yields the pure vibronic component (Fig. 3 inset, bottom trace). The distances between the neighboring peaks are plotted against an arbitrary chosen sequential number of the vibronic band (Fig. 3, diamonds). The least squares linear regression line was calculated (Fig. 3, the solid line).

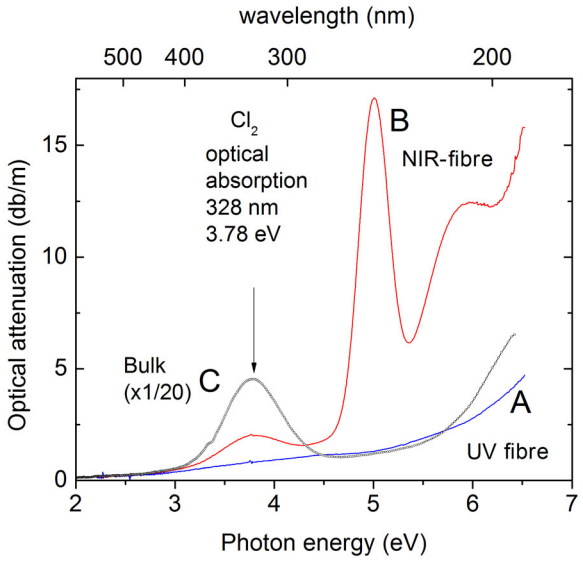

Fig. 2. Optical attenuation spectra of studied samples. (A) UV-optimized optical fibre waveguide; (B) visible to near-infrared range optimized optical fibre; (C) bulk sample of dry synthetic glassy SiO_2. The amplitude of the 3.78 eV band for NIR-fibre is 1.35 db/m (0.00311 cm^{-1}) and 74 db/m (0.17 cm^{-1}) for the bulk sample. The band at 5.0 eV is due to divalent Si ("SiODC"), the band at 5.8 eV is due to Si dangling bonds ("E′ centres").

PL excitation (PLE) spectra of the bulk sample are shown in Fig. 4. The PLE spectra, measured for each separate vibronic PL sub-band (inset of Fig. 3) nearly coincide (Fig. 4, top). The absence of correlation between the excitation and emission energies is further illustrated by the symmetric shape of the 2D excitation/emission map (Fig. 4, bottom).

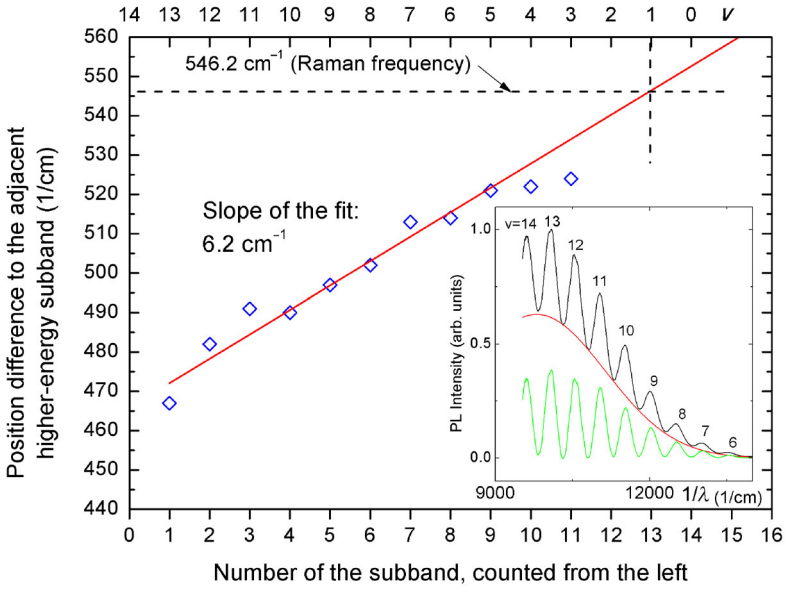

Fig. 3. Photoluminescence spectrum of interstitial Cl_2 molecules in glassy SiO_2, measured at T = 13 K and excitation 473 nm (inset, top curve), the approximation of its unstructured part by Gaussian (inset, middle curve) and the difference spectrum, showing pure vibronic sub-bands (inset, bottom). The hollow diamonds show the differences between the positions of the adjacent sub-bands. The crossing point of linear regression fit line with the line drawn at the Raman frequency corresponds to the vibrational quantum number v = 1 (upper X scale). This reference point is used to assign v values to the sub-bands in the inset.

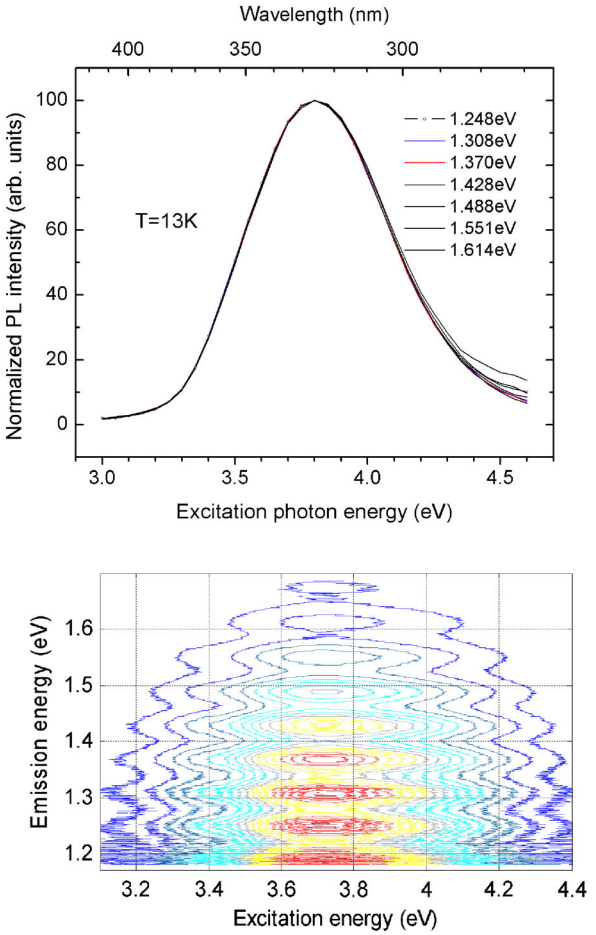

Fig. 4. Excitation spectra of interstitial Cl_2 in bulk SiO_2 sample at 13 K, measured at different PL emission energies. Top: excitation spectra for individual vibronic bands (bands with v = 13 to v = 7 in the inset of Fig. 3). Bottom: excitation/emission 2D landscape map.

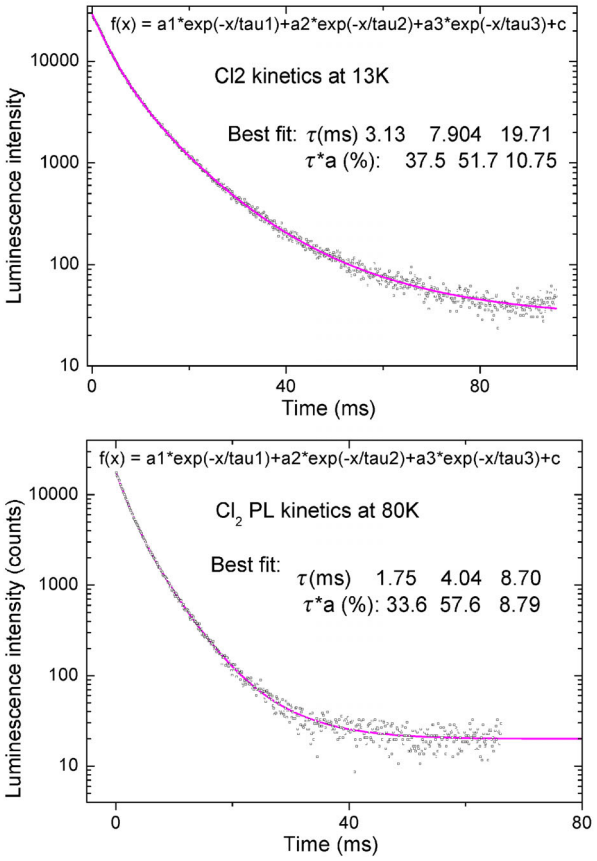

Fig. 5. Photoluminescence decay kinetics at T = 13 K (top) and 80 K (bottom) measured with 473 nm excitation and integrated for the 650–850 nm emission region. Solid lines show fit by a sum of 3 exponents.

Figure 5 shows the PL decay kinetics of the bulk sample, measured at 13 K and 80 K with a 473 nm excitation, and the non-linear least squares fits by the sum of 3 exponents. Alternative fit models by 1 or 2 exponents or by stretched exponent gave worse results. Increasing the exponent count to 4 did not increase the accuracy. The proportion between the contributions of the 3 exponents remained roughly the same as the temperature was increased from 13 K–100 K.

The PL spectra of the "UV"-type optical fibre waveguide did not show any luminescence in NIR region both at room temperature and after its immersion in liquid N_2 (78 K). In contrast, "NIR" type fibre showed very strong NIR luminescence after cooling to 78 K (Fig. 6A). The time-resolved spectrum (Fig. 6B) and its difference to the CW spectrum (Fig. 6C) reveal that the emission shifts to larger energies at longer delays.

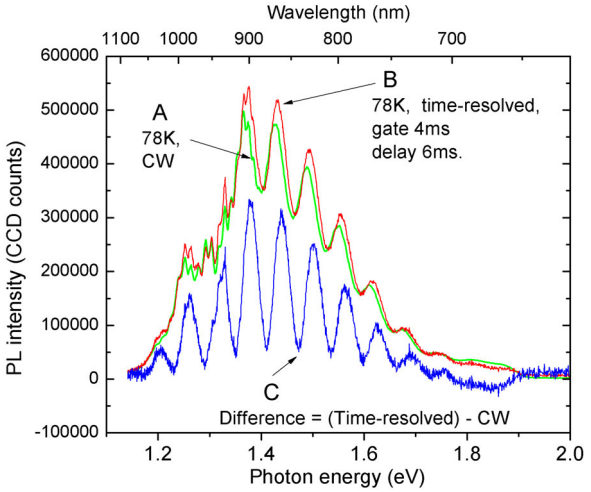

Fig. 6. Comparison between the photoluminescence spectra of optical fibre waveguide ("NIR" type), measured in CW-mode (A) and time-resolved mode (B). The time-resolved spectrum is arbitrary normalized to match the CW spectrum. Difference spectrum (C) illustrates the blue-shift of the time-delayed emission. The fine spectral features at $\lambda > 850$ nm are experimental artefacts (see the Materials and methods section).

4. DISCUSSION

4.1. Anharmonicity and zero-phonon energy

The linear increase of the distance between the neighboring vibronic bands, evident in the plot of Fig. 3 is typical for the coupling of PL emission transition to slightly anharmonic vibration mode. In the Morse potential model [10], the energies *E(v)* of the vibronic bands in PL spectrum are given by

$$E(v) = E_0 - hc\left[\omega\left(v+\tfrac{1}{2}\right) - \omega\chi\left(v+\tfrac{1}{2}\right)^2\right], \qquad (1)$$

where v is the ground state vibrational quantum number, E_0 is the excited-state zero-phonon energy, ω is the ground-state harmonic vibration frequency (in cm^{-1}units) and χ is the anharmonicity constant. The slope of the fit, $2\omega\chi$, is 6.2 cm^{-1}, giving anharmonicity parameter $\omega\chi = 3.1$ cm^{-1}. Extrapolating the fit on Fig. 3 up to the independently measured Raman frequency of interstitial Cl_2 in SiO_2 (546.2 cm^{-1} [6]), gives the number of the corresponding sub-band (Fig. 3, bottom scale) as $12.98 \approx 13$. This sub-band has vibrational quantum number $v = 1$ and subsequently, v values can be assigned to the all lower energy sub-bands (Fig. 3, top scale and the inset). This assignment of v-numbers is similar to one made for Cl_2 molecule in Ar cryocrystal matrix [11]. The natural isotope abundance of Cl_2 molecules is ^{35}Cl–^{35}Cl: 57.4%, ^{35}Cl–^{37}Cl: 36.7%, ^{37}Cl–^{37}Cl: 5.9%. If isotope-weighted averages of the positions of the sharp vibronic lines observed in [11] are calculated, their values differ less than 50 cm^{-1} from the respective positions of sub-bands measured for Cl_2 in glassy SiO_2 (Fig. 3). Zero-phonon ($v = 0$) line (ZPL) position, determined from the fit is at 16732 cm^{-1} (2.074 eV, 597.6 nm). ZPL is obviously unobservable, since the Huang–Rhys factor, the average number of vibrational quanta, created during relaxation to the ground state is $S \approx 13$ and ZPL intensity is proportional to exp(–S).

4.2. Nature of the spectral broadening

Compared to the narrow-line PL spectra of Cl_2 in inert gas crystals (FWHM<8 cm^{-1}) [11,12], the PL spectra of Cl_2 in SiO_2 are significantly broadened. Two origins of the broadening are possible: homogeneous broadening due to a strong interaction with SiO_2 matrix phonons and inhomogeneous broadening due to different Cl_2 interstitial sites in amorphous SiO_2 matrix. The homogeneous broadening surely plays a role, since the phonon energies in SiO_2 are much higher (up to 1300 cm^{-1}) than in Ar crystals (<75 cm^{-1} [13]). At the first glance, the observed (Fig. 4) complete absence of any spectral shifts in PL emission when excitation photon energy is changed, could corroborate that assumption and indicate a relatively small inhomogeneous broadening. However, the excitation at energies above 3 eV goes to a repulsive state (A $^1\Pi_u$) [14]. The luminescence from the lower-lying triplet state (a $^3\Pi_u$) can occur at this excitation only because Cl_2 is prevented from dissociation by the cage effect of the surrounding SiO_2 matrix [6]. Under these conditions, any correlation between the excitation and emission energies, which is characteristic to inhomogeneously broadened luminescence, may be lost.

A clue for the relative size of inhomogeneous broadening can be found from the kinetics and time-resolved measurements. An analysis of the decay kinetics (Fig. 5) indicates the presence of several exponents or of a continuous distribution of decay constants. In contrast, in Ar matrix a single lifetime ($\tau = 76$ ms) was found, independent of temperature or of the Cl isotopic species [12]. The time resolved spectra (Fig. 6) show a clear blue shift of the spectra by ≈40 cm^{-1}at longer decay times, the difference spectrum (Fig. 6 C) is shifted by ≈80 cm^{-1}. These shifts are, however, relatively small compared to the halfwidth of the vibronic bands (240 cm^{-1}). Evidently, the main broadening comes from electron-phonon coupling and ≈10–20% comes from different environments of Cl_2 in the interstices of glassy SiO_2.

4.3. Detection threshold of Cl_2 in optical fibre waveguides

The PL spectrum of Cl_2 in optical fibre (Fig. 6A) was obtained for an optical fibre, containing 8×10^{15} Cl_2/cm^3, as calculated from the amplitude of the 3.73 eV absorption band (Fig. 2) and Cl_2 absorption cross section, 2.58×10^{-19} cm^2 [7]. The intensity of the PL, obtained at the total exposure time of 18 s (30 × 0.6 s) was well over 10^3 times above the noise level. Further, the exposure time, the excitation power (1 mW) and the length of the cooled section of the fibre (0.80 m) all can be easily increased by a factor of 10. This gives an additional dynamic range of order $10^3 \times 10 \times 10 \times 10 = 10^6$ times as compared to the present measurement and gives the detectivity estimate of better than 10^{10} Cl_2/cm^3. It is much better than the typical sensitivity (≈ 10^{17} Cl/cm^3) of electron microprobe (EMPA) analysis. However, the PL technique is sensitive only to molecular Cl_2, while EMPA detects all forms of chlorine. This can provide an opportunity to follow the early stages of formation of Cl_2 in photo-radio-chemical reactions [5] in the types of fibres initially containing chlorine as SiCl groups or in other chemical forms.

5. CONCLUSIONS

Following our recent work [6], this study provides further spectroscopic details on photoluminescence of interstitial Cl_2 in glassy SiO_2. This PL represents one of the very few observations of vibronic structures in the luminescence of pure or light-element doped glassy SiO_2. The other instances comprise interstitial O_2, dangling oxygen bonds [8], interstitial sulphur S_2 molecules [15] and not yet identified silicon-oxygen-related species in silica nanoparticles [16]. The luminescence of Cl_2 is easily distinguished from other common PL bands in glassy SiO_2 [8] by its spectral position, shape and lifetime. Given the importance of chlorine in the manufacturing processes of glassy SiO_2 and optical fibres, this PL has potential application for monitoring Cl-related processes in SiO_2.

ACKNOWLEDGEMENTS

The support from Latvian Research Program IMIS 2, project "Photonics and materials for photonics" is acknowledged. K.K. was partially supported by the Collaborative Research Project of Materials and Structures Laboratory, Tokyo Institute of Technology. The publication costs of this article were covered by the Estonian Academy of Sciences and the University of Tartu.

REFERENCES

1. Chiodini, N., Lauria, A., Lorenzi, R., Brovelli, S., Meinardi, F., and Paleari, A. Sol–gel strategy for self-induced fluorination and dehydration of silica with extended vacuum ultraviolet transmittance and radiation hardness. *Chem. Mater.*, 2012, **24**, 677–681.
2. Awazu, K., Kawazoe, H., Muta, K., Ibuki, T., Tabayashi, K., and Shobatake, K. Characterization of silica glasses, sintered under Cl_2 ambients. *J. Appl. Phys*., 1991, **69**, 1849–1852.
3. Girard, S., Ouerdane, Y., Origlio, G., Marcandella, C., Boukenter, A., Richard, N., Baggio, J., Paillet, P., Cannas, M., Bisutti, J., Meunier, J. P., and Boscaino, R. Radiation effects on silica-based preforms and optical fibers–I: experimental study with canonical samples. *IEEE Trans. Nucl. Sci.*, 2008, **55**, 3473–3482.
4. Cheremisin, I. I., Ermolenko, T. A., Evlampiev, I. K., Popov, S. A., Turoverov, P. K., Golant, K. M., and Zabezhajlov, M. O. Radiation-hard KS–4V glass and optical fiber, manufactured on its basis, for plasma diagnostics in ITER. *Plasma Devices Oper.*, 2004, **12**, 1–9.
5. Kajihara, K., Hirano, M., Skuja, L., and Hosono, H. Reactions of SiCl groups in amorphous SiO_2 with mobile interstitial chemical species: formation of interstitial Cl_2 and HCl molecules, and role of interstitial H_2O molecules. *J. Appl. Phys.*, 2005, **98**, 043515(1–9).
6. Skuja, L., Kajihara, K., Smits, K., Silins, A., and Hosono, H. Luminescence and Raman detection of molecular Cl_2 and ClClO molecules in amorphous SiO_2 matrix. *J. Phys. Chem. C*, 2017, **121**, 5261–5266.
7. Maric, D., Burrows, J. P., Meller, R., and Moortgat, G. K. A study of the UV-visible absorption spectrum of molecular chlorine. *J. Photochem. Photobiol. A*, 1993, **70**, 205–214.
8. Skuja, L., Hirano, M., Hosono, H., and Kajihara, K. Defects in oxide glasses. *Phys. Stat. Sol. C*, 2005, **2**, 15–24.
9. Girard, S., Kuhnhenn, J., Gusarov, A., Brichard, B., van Uffelen, M., Ouerdane, Y., Boukenter, A., and Marcandella, C. Radiation. Effects on silica-based optical fibers: recent advances and future challenges. *IEEE Trans. Nucl. Sci*., 2013, **60**, 2015–2036.
10. Morse, P. M. Diatomic molecules according to the wave mechanics. II. Vibrational levels. *Phys. Rev*., 1929, **34**, 57–64.
11. Ault, B. S., Howard, W. F., Jr., and Andrews, L. Laser-induced fluorescence and Raman spectra of chlorine and bromine molecules isolated in inert matrices. *J. Mol. Spectrosc.*, 1975, **55**, 217–228.
12. Bondybey, V. E. and Fletcher, C. Photophysics of low lying electronic states of Cl_2 in rare gas solids. *J. Chem. Phys.*, 1976, **64**, 3615–3620.
13. Occelli, F., Krisch, M., Loubeyre, P., Sette, F., Le Toullec, R., Masciovecchio, C., and Rueff, J.-P. Phonon dispersion curves in an argon single crystal at high pressure by inelastic x-ray scattering. *Phys. Rev. B*, 2001, **63,** 224306(1–8).
14. Peyerimhoff, S. D. and Buenker, R. J. Electronically excited and ionized states of the chlorine molecule. *Chem. Phys.*, 1981, **57**, 279–296.
15. Zavorotny, Yu. S., Lutsko, E. V., Rybaltovskii, A. O., Chernov, P. V., Sokolov, V. O., and Khrapko, R. R. Color centers in sulfur-doped silica glass: spectroscopic manifestations of an interstitial molecule S_2. *Glass Phys. Chem.*, 2001, **27**, 331–336.
16. Spallino, L., Vaccaro, L., Sciortino, L., Agnello, S., Buscarino, G., Cannas, M., and Gelardi, F. M. Visible-ultraviolet vibronic emission of silica nanoparticles. *Phys. Chem. Chem. Phys.*, 2014, **16**, 22028–22034.

Kloorimolekulide luminestsents SiO_2-klaasides ja optilistes lainejuhtides

Linards Skuja, Koichi Kajihara, Krisjanis Smits, Kalvis Alps, Andrejs Silins ja Janis Teteris

SiO_2-klaas on peamine optiliste kiudmaterjalide algmaterjal. Tootmise käigus lisanduvad viimasesse klooriaatomid, mis põhjustavad materjali läbipaistvuse vähenemist UV piirkonnas. Artiklis on põhjalikult käsitletud Cl_2 lisandimolekulide SiO_2-s põhjustatud madalatemperatuurilist fotoluminestsentsi (FL) lähedases infrapunases piirkonnas (1,23 eV), lähtudes viimases esineva Cl_2 FL-i vibroonse spektri mitteharmoonilisusest. Spektri vibroonsed ribad on laienenud tänu klaasilise korrapäratuse poolt lisandunud footoni ja võrevõnkumiste vahelistele interaktsioonidele. Huangi-Rhysi faktor on ≈13. FL-i kustumisaeg temperatuurivahemikus 100–13 K on 1 ja 10 ms vahel ning seda kirjeldab kolmeosaline eksponent. Tõstes temperatuuri 13 K-lt vedela lämmastiku temperatuurini, säilitab Cl_2 FL-i suhteliselt kõrge kvantefektiivsuse ja iseloomuliku kuju. Viimane võimaldab kasutada spektrit kõrge tundlikkusega diagnoosivahendina Cl_2 lisandite detekteerimiseks optilistes lainejuhtides. Optiliste fiibrite aeglahutusega mõõtmised näitavad, et detekteerimise tundlikkuse piir on 10^{10} Cl_2/cm^3.

Institute of Solid State Physics, University of Latvia as the Center of Excellence has received funding from the European Union's Horizon 2020 Framework Programme H2020-WIDESPREAD-01-2016-2017-TeamingPhase2 under grant agreement No. 739508, project CAMART²